Cell Transplantation, Vol. 26, pp. 879–890, 2017

0963-6897/17 $90.00 + .00
DOI: https://doi.org/10.3727/096368916X693789
E-ISSN 1555-3892
www.cognizantcommunication.com

Human Bone Progenitor Cells for Clinical Application: What Kind of Immune Reaction Does Fetal Xenograft Tissue Trigger in Immunocompetent Rats?

Tanja C. Hausherr,* Katja Nuss,† Eric Thein,‡ Lee A. Applegate,§ and Dominique P. Pioletti*

*Laboratory of Biomechanical Orthopedics, Ecole Polytechnique Fédéreale de Lausanne, Lausanne, Switzerland
†Musculoskeletal Research Unit, Vetsuisse Faculty, University of Zürich, Zürich, Switzerland
‡Orthopedic and Traumatology Department, University Hospital of Lausanne (CHUV), Lausanne, Switzerland
§Regenerative Therapy Unit, Plastic and Reconstructive Surgery, University Hospital of Lausanne (CHUV), Lausanne, Switzerland

The potential of human fetal bone cells for successful bone regeneration has been shown in vivo. In particular, it has been demonstrated that the seeding of these cells in porous poly-(L-lactic acid)/β-tricalcium phosphate scaffolds improved the bone formation compared to cell-free scaffolds in skulls of rats. However, even if the outcome is an improvement of bone formation, a thorough analysis concerning any immune responses, due to the implantation of a xenograft tissue, is not known. As the immune response and skeletal system relationship may contribute to either the success or failure of an implant, we were interested in evaluating the presence of any immune cells and specific reactions of human fetal cells (also called human bone progenitor cells) once implanted in femoral condyles of rats. For this purpose, (1) cell-free scaffolds, (2) human bone progenitor cells, or (3) osteogenic human bone progenitor cells within scaffolds were implanted over 3, 7, 14 days, and 12 weeks. The key finding is that human bone progenitor cells and osteogenic human bone progenitor cells do not trigger any particular specific immune reactions in immunocompetent rats but are noted to delay some bone formation.

Key words: Bone tissue engineering (BTE); Scaffold; Cell therapy; Human bone progenitor cells (hBPCs); Immune response

INTRODUCTION

The high demand of bone tissue engineering scaffolds due to bone trauma, nonunions, or resection of tumors creates a great challenge in the field of bone regeneration[1–3]. Problems related to the use of auto- and allografts, such as limited supply, donor site morbidity, scarring, surgical risk, risk of infections, cost issues, and logistical challenges in creating bone banks[4–7], have led to a growing interest in the field of bone tissue engineering (BTE) in the last three decades[6]. Therefore, the current aim of BTE, which matches the needs of the orthopedic medicine, is to obtain bone healing in the shortest time frame, with the best possible functional recovery associated with the least complications[8]. To achieve this goal, different approaches have been used, in which synthetic bone substitutes that have similar mechanical properties of bone in addition to allowing a sufficient vascularization are combined with either osteogenic engineered cells, morphogenic signals, or mechanical stimulations[6,9–12].

Several approaches combining biomaterials with bone marrow preparations[13,14], bone marrow-derived mesenchymal stem cells (BM-MSCs)[15,16], or osteoblasts[6] were described to be promising for BTE. Furthermore, the potential of human fetal cells for a successful engineered regeneration of adult skeletal tissue has been shown in vitro and in vivo[17,18]. In these in vitro studies, it has been shown that human fetal cells, also called human bone progenitor cells (hBPCs), could be of great interest for bone research due to their rapid growth rate, advanced osteogenesis development, and ability to differentiate into mature osteoblasts. For this reason they are also referred to as osteogenic human bone progenitor cells (hOBPCs). In a later in vivo study, Montjovent et al.[19] evaluated the effect of hBPCs in combination with porous poly-(L-lactic acid)/β-tricalcium phosphate (PLA/β-TCP) scaffolds. The cell-seeded scaffolds were implanted in skulls of rats, and a histological qualitative evaluation of bone repair at 12 days and at 6 and 12 months after implantation

Received August 30, 2016; final acceptance February 8, 2017. Online prepub date: November 21, 2016.
Address correspondence to Professor Dominique P. Pioletti, Laboratory of Biomechanical Orthopedics, Ecole Polytechnique Fédérale de Lausanne, Station 9, CH-1015 Lausanne, Switzerland. Tel: +41 (0) 21 693 83 41; E-mail: dominique.pioletti@epfl.ch

was performed. The ossification along the dura and the porous ossification in scaffolds were analyzed, and it was found that the cell-seeded scaffolds improved the bone formation compared to cell-free scaffolds in this model.

Even though the final outcome was an improvement of bone formation, a thorough analysis concerning associated immune responses with the implantation of a xenograft tissue is necessary. This kind of information is especially relevant to the envisioned clinical application of transplanting hBPCs into different patients, which will then represent an allograft. As the immune response and skeletal system relationship may contribute to either the success or failure of an implant[20], we therefore investigated what kind of immune response would be potentially triggered in an early stage of implantation of scaffolds seeded with hBPCs or without any cells as a control. Furthermore, hOBPC-seeded scaffolds were studied as well to get more information on the behavior of the differentiated and mineralized state of hBPCs. Because these later cells may mature in vivo and become hOBPCs, a different immunological reaction could be triggered by the host. As little information is yet available concerning the difference in behavior between hBPCs and hOBPCs in vivo, we wanted to evaluate whether these different cell lineages have an influence on host immunity after they are first transplanted and on the long term. For this purpose, each scaffold group was implanted in both femoral condyles of female Wistar rats, and a tissue analysis was performed after 3, 7, and 14 days as well as after 12 weeks of implantation. In addition to the evaluation of immune reaction, the localization and eventual migration of the cells were of interest.

MATERIALS AND METHODS

Cell Culture

The hBPCs used in this study were obtained from a registered biobank (CHUV Lausanne, Switzerland), and cell bank development was approved by the local ethics committee (Protocols 51/10). The bone cells were harvested from a tissue donation under the registered Transplantation Program (fetal bone tissue of 15 weeks gestational age following a voluntary interruption of pregnancy) and treated as described elsewhere[19]. Briefly, hBPC cultures were established by rinsing the tissue first with phosphate-buffered saline (PBS; Thermo Fisher Scientific, Waltham, MA, USA) containing penicillin–streptomycin (Thermo Fisher, for washing only). Afterward, bone samples were mechanically dissociated with a scalpel blade and transferred to 10-cm culture-grade plates where cell outgrowth was seen within 2 to 5 days under normal culture conditions: Dulbecco's modified Eagle's medium (DMEM; Invitrogen, Carlsbad, CA, USA), 10% fetal calf serum (FCS; Sigma-Aldrich, St. Louis, MO, USA), and 2 mM L-glutamine (Invitrogen). For cell expansion, the cells were cultured in T75 flasks (TPP® tissue culture flask; Sigma-Aldrich) in a standard culture medium composed of DMEM, supplemented with 10% (v/v) fetal bovine serum (FBS; Thermo Fisher Scientific) and 1% (v/v) L-glutamine (200 mM). They were maintained in culture at 37°C in 5% CO_2 atmosphere with culture media changed twice weekly and were passaged when they reached 80% confluency. When the hOBPCs were used for in vivo experiments, the following osteogenic differentiation medium was prepared: α-minimum essential medium Eagle (MEM; Gibco, Thermo Fisher Scientific), 10% (v/v) FBS, 1% (v/v) L-glutamine (200 mM), 1% (v/v) vitamin C (5 mg/ml; Sigma-Aldrich), 1% (w/v) β-glycerophosphate (500 mM; Sigma-Aldrich), and 1% (w/v) dexamethasone (1 mM; Sigma-Aldrich). The cells were first plated in a standard culture medium and then exposed to the osteogenic differentiation medium at the third day of culture. The medium was renewed three times a week over 2 weeks.

Scaffold Fabrication

The scaffolds used in this work were developed in collaboration with the Laboratory of Polymer and Composite Technology (LTC, EPFL, Lausanne, Switzerland). The processing and properties analysis of the scaffolds were carried out as described elsewhere[21]. In short, the scaffolds were made of polylactic acid (PLA; Boehringher Ingelheim, Ingelheim am Rhein, Germany) and β-TCP ceramic powder (Sigma-Aldrich), which were mixed (5%, w/w) and melt extruded using a microcompounder (Xplore, Geleen, Netherlands). Afterward, the melt-extruded product was foamed with supercritical CO_2 in a custom-made high-pressure chamber. Once the CO_2 was dissolved in PLA, foaming was achieved by sudden gas release, which induces bubble nucleation and formation. The rising porous structure was then fixed by simultaneously cooling and depressurizing the high-pressure chamber[19]. The final volume of synthetic composite PLA/5% β-TCP used for the in vivo study was machined into cylinders of 3-mm height and 3-mm diameter.

Scaffold Preparation and Seeding

The PLA/5% β-TCP scaffolds were sterilized by ethylene oxide at the CHUV (Lausanne, Switzerland). Prior to the cell seeding, the scaffolds were wet and sonicated (Ultrasonik; Ismatec SA, Werheim, Germany) for 20 min in order to avoid the entrapment of micro-air bubbles in the scaffold. The cells were seeded at passage 4 at a concentration of 0.5×10^6 cells/scaffold in PLA/5% β-TCP scaffolds using a pressure-driven technique. Once seeded, the scaffolds were placed on a rotating platform, allowing a homogeneous cell distribution inside the scaffold. For the in vivo study, we distinguished between three

different types of scaffolds: cell-free (CF), seeded with hBPC (CS), and seeded with hOBPC (OCS) scaffolds. In the case of CF scaffolds, the scaffolds were wet with 0.9% NaCl solution (B. Braun, Melsungen, Germany) for the sonication and then left in 200 µl of 0.9% NaCl solution for 72 h in the incubator before implantation. For the CS scaffold, the scaffolds were wet with standard culture medium and were seeded with hBPCs 3 days before implantation, whereas OCS scaffolds were seeded with hBPCs 2 weeks before implantation for in vivo experimentation. The medium of OCS scaffolds was changed three times a week with osteogenic differentiation medium to obtain hOBPC-seeded scaffolds. Just before implantation, every scaffold was washed three times with sterile 0.9% NaCl solution.

Study Design

The in vivo study included three experimental groups defined by the implanted PLA/5% β-TCP scaffold type (CF, CS, and OCS). Each type of scaffold was implanted in a predrilled hole in both femoral condyles of rats. In each experimental group, 15 rats were operated. Three to four of the rats were euthanized either at 3, 7, and 14 days or at 12 weeks after implantation in order to detect any immune reaction possibly due to the use of hBPCs and hOBPCs. Blood samples were collected before the surgical intervention and before euthanasia to make a white blood cell count analysis at time points 3, 7, and 14 days of implantation.

Surgical Procedure

All animal procedures were performed with the approval of the local animal care and use committee (License No. 2631.0; EXPANIM, SCAV, Epalinges, Switzerland). Female Wistar rats (280–300 g) were purchased from Janvier Labs (Saint-Berthevin, France). For implanting scaffolds in femoral condyles of rats, the protocol was slightly adapted from Roshan-Ghias et al.[22,23]. The rats were anesthetized with isoflurane gas (induction: 5% at 2.0 L/min, during surgery: 2.5% at 0.8 L/min; Piramal Enterprise Ltd., Bombay, India). After anesthesia induction, blood was taken from the rat's tail. The animal's legs were shaved, and buprenorphine (0.03 mg/kg/day; Temgesic®; Reckitt Benckiser AG, Wallisellen, Switzerland) was injected subcutaneously as analgesia. The animal was then situated on a custom-made table to fix and to stabilize the leg. After 1- to 2-cm skin incision on the lateral side of the distal femoral end and muscle dissection[24], a hole with a diameter of 3 mm and height of 3 mm was drilled in the condyle underneath the growth plate using a motorized dentist's drill (DEC 100; Nobel Biocare, Karlskoga, Sweden). Before and after the drilling, the site of implantation was cooled and rinsed with 0.9% NaCl. Afterward, either a CF, CS, or OCS PLA/5% β-TCP scaffold was implanted by press fitting it inside the drilled hole. The muscles and skin were then closed with synthetic absorbable sterile surgical sutures [coated VICRYL® (polyglactin 910); 5-0; Ethicon Inc., Somerville, NJ, USA] with interrupted subcutaneous stitches [coated VICRYL® (polygalctin 910); 5-0]. The animal was then prepared to make the same surgical intervention on the contralateral femur. Buprenorphine was injected subcutaneously every 8 h for the first 72 h after surgery for pain relief completed by the addition of paracetamol (Dafalgan; 500 mg effervescent tablet; UPSA Bristol-Myers Squibb SA, Baar, Switzerland) to the drinking water of the rats for 1 week. Intracardiac blood samples were collected before the euthanasia of rats at 3, 7, and 14 days after scaffold implantation. All rats were euthanized with an intracardiac pentobarbital (<200 mg/kg; Esconarkon; Streuli Pharma SA, Uznach, Switzerland) injection.

Blood Smear Staining and Leukocyte Count

After rat blood collection, a drop of blood was smeared on a glass slide (Polysciences Inc., Warrington, PA, USA). The samples were then stained with Hemacolor® Rapid staining (Merck Millipore Corporation, Billerica, MA, USA) according to the manufacturer's instructions. This staining is based on the Pappenheim staining technique, which enables the differential counts of white blood cells including lymphocytes, monocytes, nonsegmented neutrophils, juvenile neutrophils, segmented neutrophils, eosinophils, and basophils based on their morphology. Two separate investigators counted 100 cells for each sample, and the results were averaged for the statistical analysis.

Histology

After blood sample collection, the animals were directly euthanized, and femur distal parts were dissected and fixed in 4% paraformaldehyde (PFA; Sigma-Aldrich) solution for approximately 1 day. The samples were dehydrated by immersing them in a series of ethanol (EtOH; VWR International, Dietikon, Switzerland) solutions with ascending concentration (70%, 80%, 90%, 96%, and 100%) as described elsewhere[24]. Each immersion lasted for 24 h. The samples were then cleared 1×24 h in toluene (VWR International) and then again in a refreshed toluene solution for 1×48 h. Afterward, two thirds of the femur samples were embedded by infiltration with methylmethacrylate (MMA; 100 ml; Sigma-Aldrich) and 0.5% bis(tert-butylcyclohexyl)peroxydicarbonate (Perkadox 16; Dr Grogg Chemie AG, Deisswil, Switzerland) at 4°C for 5 days. For polymerization, 100 ml of MMA, 20–25 ml of dibutyl phthalate (DBP; Sigma-Aldrich), and 1% of Perkadox 16 (Dr Grogg Chemie AG) were prepared, and the samples were polymerized at room temperature (RT) over 3 weeks. The left one third of the

samples were embedded in Technovit 9100 (Heraeus Kulzer GmbH, Hanau, Germany) according to the manufacturer's instructions. The Technovit 9100 has a polymerization temperature between −4°C and 0°C, which allows the preservation of DNA and RNA. After polymerization, MMA- and Technovit 9100-embedded samples (referred to as resin blocks) were cut with a diamond-coated inner diameter saw (Leica SP 1600; Leica Microsystems, Wetzlar, Germany) into slices of around 180-µm thickness (referred to as thick slice). Four to five of these MMA preparations were cut and attached to custom-made opaque o-methyl methacrylate (OMMA) microscope slides (Semadeni AG, Ostermundigen, Switzerland) with acrylic glue (Loctite 401; Henkel, Düsseldorf, Germany). They were then ground to around 80- to 100-µm thicknesses with a grinding machine (Pedemax-2; Struers, Willich, Germany) before staining. The rest of the Technovit 9100 resin blocks were cut with a microtome (HM325; Microm International GmbH, Walldorf, Germany) into slices of around 10 µm (referred to as thin slide). They were attached on silane glass slides (Polysciences) with 90% EtOH. Finally, the slides were clamped at 37°C over 48 h and released for at least 2 h at RT before staining.

The surface of the thick slides was etched with 1% formic acid (AppliChem, Darmstadt, Germany) before being stained with 0.1% toluidine blue (VWR International). For the thin slides, the resin was deplastified with a series of different bathes. First, the slides were immersed three times for 20 min in toluene (VWR International), followed by hydration in a series of EtOH with a descending concentration (100%, 90%, 80%, and 70%); slides were immersed for 10 min each. The slides were finally put in deionized water before human-specific Alu in situ hybridization (Alu-ISH) for the detection of hBPCs. Positive controls, provided by the histology facility, were simultaneously run with our samples. The positive controls were human tissue (heart, skin, or demineralized bone) embedded in paraffin. The Alu-ISH was performed using a fluorescein isothiocyanate (FITC)-labeled human-specific Alu probe (Roche Diagnostics, Rotkreuz, Switzerland). The Alu-ISH on rat femur resin sections was done using the fully automated instrument Ventana Discovery xT (Roche Diagnostics). All steps, except the deplastification described previously, were performed on the machine with Ventana solutions (Roche Diagnostics), as described elsewhere[25,26]. Briefly, deplastified and rehydrated resin sections were pretreated with the RiboMap kit (Roche Diagnostics) and with protease 1 (Roche Diagnostics) for 8 min at 37°C. The human-specific Alu probe was hybridized for 1 h at 47°C. Sections were then washed three times with Ribowash [2× saline sodium citrate (SSC) buffer with 0.1% sodium dodecyl sulfate (SDS); Roche Diagnostics] for 8 min at 45°C. After incubation with an anti-FITC biotin (1:300; Jackson ImmunoResearch Laboratories, West Grove, PA, USA), chromogenic revelation was performed with the BlueMap kit for 2 h. Counterstain using Nuclear Fast Red (Carl Roth GmbH & Co. KG, Karlsruhe, Germany) was performed on a Tissue-Tek® Prisma® automate (Sakura Finetek, Alphen aan den Rijn, Netherlands) for 5 min. Slides were mounted with a xylene-based glue (Sakura Finetek).

Images were taken with an upright light microscope with different magnifications (DM 5500; Leica Microsystems). Based on the stained sections, a qualitative evaluation was performed, where cellular events were interpreted. The osteoblast activation, shape, and the presence of inflammatory cells (neutrophils, macrophages, lymphocytes, plasma cells, multinuclear giant cells, and fibrous capsule) were observed and commented. The percentage of fibrous tissues and maturity of the bone were evaluated inside the scaffold.

Statistical Analysis

The results obtained for the leukocyte count were analyzed using a *t*-test. At each time point, it was tested whether there was a significant difference between the different scaffolds ($n = 3–4$). A value of $p < 0.05$ or $p < 0.01$ was considered as significant. All statistical analyses were done in R (R Development code Team 2010, Auckland, New Zealand).

RESULTS

Cell Visualization and Localization

For the localization of hBPCs inside and around the scaffold with an eventual observation of a migration pattern outside the scaffold over time, we used human-specific Alu elements with in situ hybridization of thin deplastified resin slides. For this application, we chose a specific resin (Technovit 9100) with a polymerization temperature around 0°C in order to avoid the DNA and RNA denaturization due to temperature. The obtained results are shown in Figure 1. Two samples out of 20 did polymerize correctly, where one of them was our first test sample (CS condition, after 4 days of implantation) and the second one was an OCS scaffold at 14 days postimplantation.

On both stained samples, hBPCs and hOBPCs were detected inside the scaffold. In the case of the CS scaffold, which was implanted for 4 days, the cells were visible in different regions inside and at the border of the scaffold (black arrow heads). They were localized inside the pores at their surface. On the left top image, we can observe a cluster of cells. On the images from the OCS scaffold, implanted for 14 days, few cells were detected, localized in pores near the border. In this case, the cells seem not to adhere at the surface of the pores but are seen inside the pores, surrounded by the extracellular matrix and other cells.

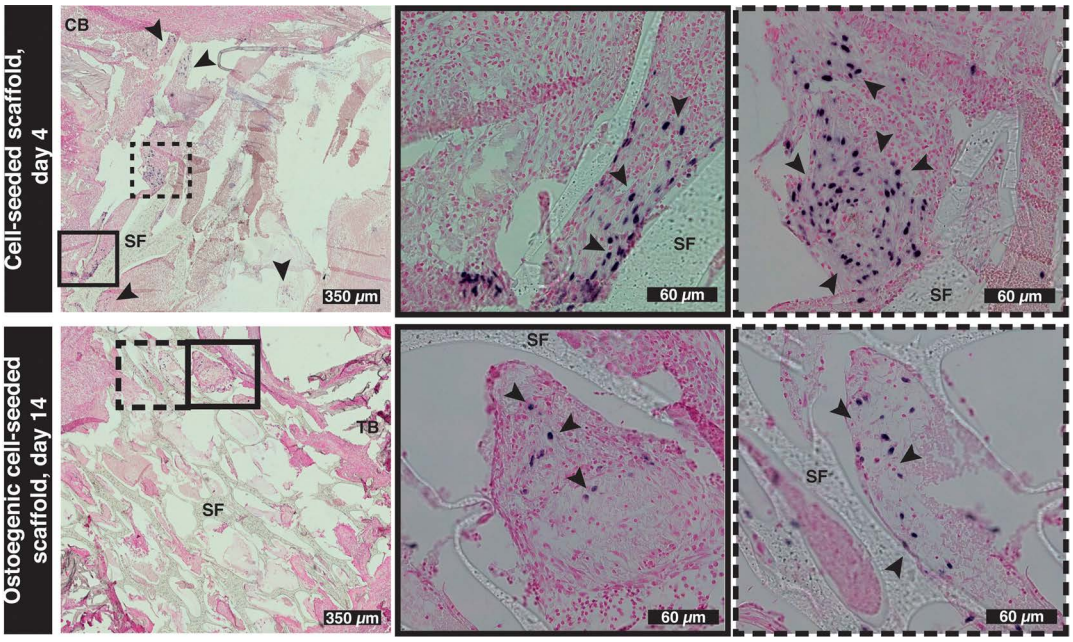

Figure 1. Alu-ISH with a counter Nuclear Fast Red stain on sections of CS scaffolds after 4 days and on sections of OCS scaffolds after 14 days of implantation. The black arrowheads indicate the hBPCs and hOBPCs (in blue) inside the scaffolds. TB, trabecular bone; CB, cortical bone; SF, scaffold; Alu-ISH, Alu in situ hybridization; CS, scaffold seeded with hBPCs; OCS, scaffold seeded with hOBPCs; hBPCs, human bone progenitor cells; hOBPCs, osteogenic human bone progenitor cells.

Hematology

The results of the differential leukocyte count after 3, 7, and 14 days of implantation are shown in Figure 2. The leukocyte count of days 3, 7, and 14 were all normalized to the leukocyte count of day 0. After 3 days of implantation, no significant differences were observed in the percentage of different white blood cells in between the scaffold conditions as presented (Fig. 2a).

Results at day 7 are presented in Figure 2b. A statistically significant increase in lymphocytes can be observed for the OCS scaffolds compared to the CF and CS scaffolds, whereas there is a decrease in monocytes and nonsegmented and juvenile neutrophils for the OCS scaffolds. The segmented neutrophils, however, augmented for the CF scaffolds compared to the CS and OCS scaffolds. The number of eosinophils and basophils stayed in all three scaffold conditions quite similarly. After 14 days of implantation for monocyte levels, one can observe a statistically significant increase between the CF and OCS scaffolds and between the CF and CS scaffolds (Fig. 2c). In general, over time, the level of lymphocytes increased for all three scaffold conditions over the 14 days, whereas the monocyte, juvenile neutrophil, and nonsegmented and segmented neutrophil levels tended to decrease.

Histology

The histology images of implanted OCS, CS, and CF scaffolds after 3, 7, and 14 days and after 12 weeks are shown in Figures 3–5, respectively. For qualitative assessment, the results are shown in Tables S1 and S2 (supplementary material available at http://infoscience.epfl.ch/record/221050). In the case of the OCS and CS scaffolds, 25%–75% and 25%–30% of fibrous tissues were present inside the scaffold over the first 14 days, respectively (Table S1). In both conditions, it partially formed at the top and around the scaffold without encapsulating the scaffold. In the case of the CF scaffolds, 10%–15% of fibrous tissue was observed inside the scaffold coming from the top of the scaffold (Table S1). After 12 weeks of implantation, 5%–15%, 5%–10%, and 10%–75% of fibrous tissues were observed in the CF, CS, and OCS scaffolds, respectively (Table S1). In the early stage of implantation, CF scaffolds were in direct contact with the surrounding bone. In all three conditions, osteoblast activation toward the scaffolds as well as newly formed bone at the bottom of the scaffold were observed over the first 14 days of implantation. Many red blood cells are visible for all three scaffold conditions, mainly at days 3 and 7 (Figs. 3–5). The neutrophils, macrophages, lymphocytes, plasma cells, and multinuclear giant cells were qualitatively rarely observed in the three scaffold conditions (Table S2). A slightly higher amount of those cells were observed in the case of the CF scaffolds compared to the CS and OCS scaffolds. For all scaffold conditions and time points, the amount of observed immune cells was in the normal range (Table S2). Inside the OCS and the

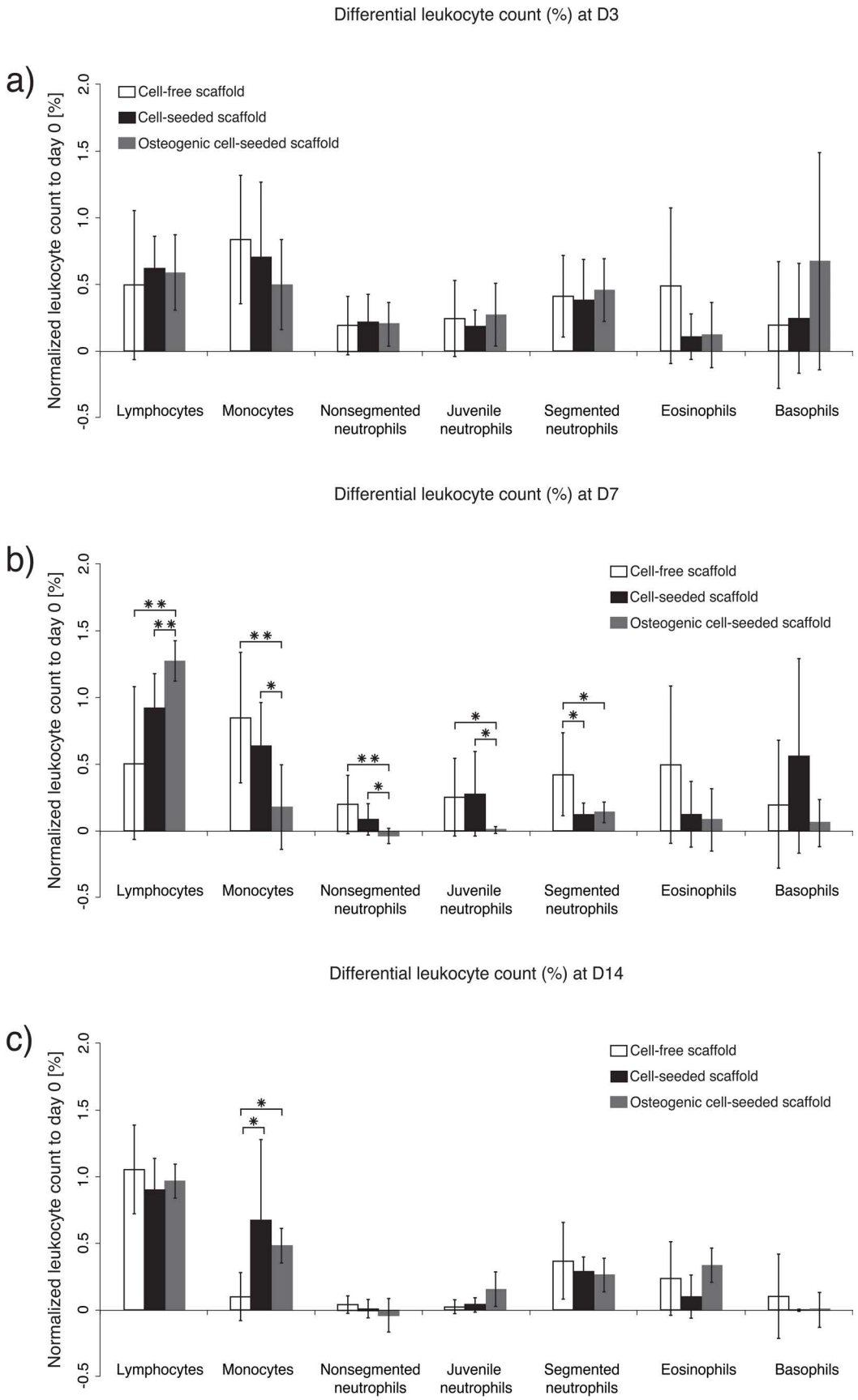

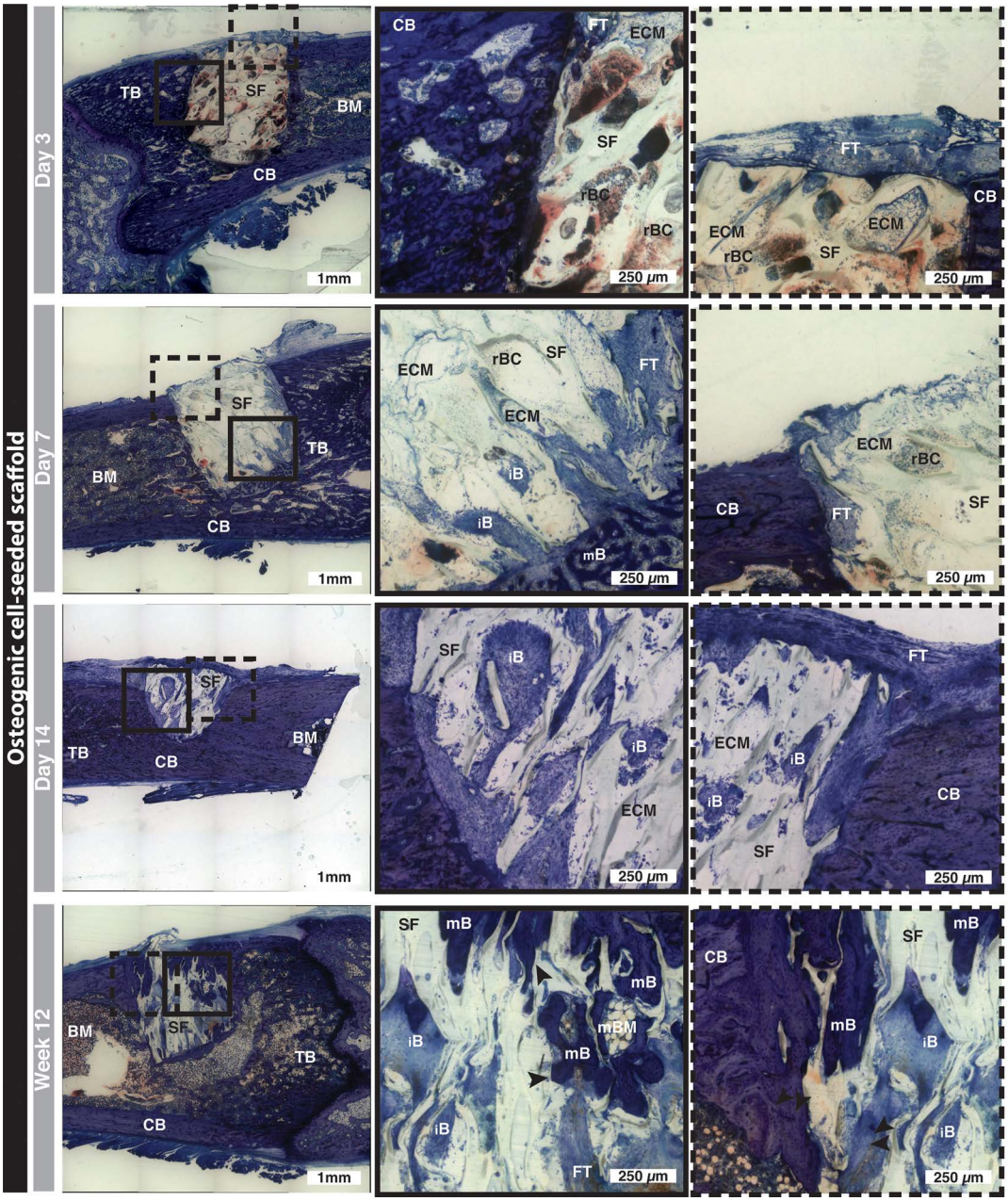

Figure 3. Toluidine blue-stained sections of OCS scaffolds after 3, 7, and 14 days and after 12 weeks of implantation. TB, trabecular bone; CB, cortical bone; BM, bone marrow; SF, scaffold; rBC, red blood cells; FT, fibrous tissue; ECM, extracellular matrix; iB, immature bone; mB, mature bone modeling; OCS, scaffold seeded with hOBPCs; hOBPCs, osteogenic human bone progenitor cells.

FACING PAGE

Figure 2. Normalized leukocyte count in blood taken after (a) 3 days, (b) 7 days, and (c) 14 days of CF, CS, and OCS scaffold implantation in femoral condyles of rats, respectively. Blood smears (with $n = 3–4$) were analyzed using the Pappenheim method. The lymphocytes, monocytes, nonsegmented, juvenile, and segmented neutrophils, eosinophils, and basophils after 3, 7, and 14 days of implantation were normalized to the one just before implantation (day 0). $*p < 0.05$ and $**p < 0.01$. CF, cell-free scaffold; CS, scaffold seeded with hBPCs; OCS, scaffold seeded with hOBPCs; hBPCs, human bone progenitor cells; hOBPCs, osteogenic human bone progenitor cells.

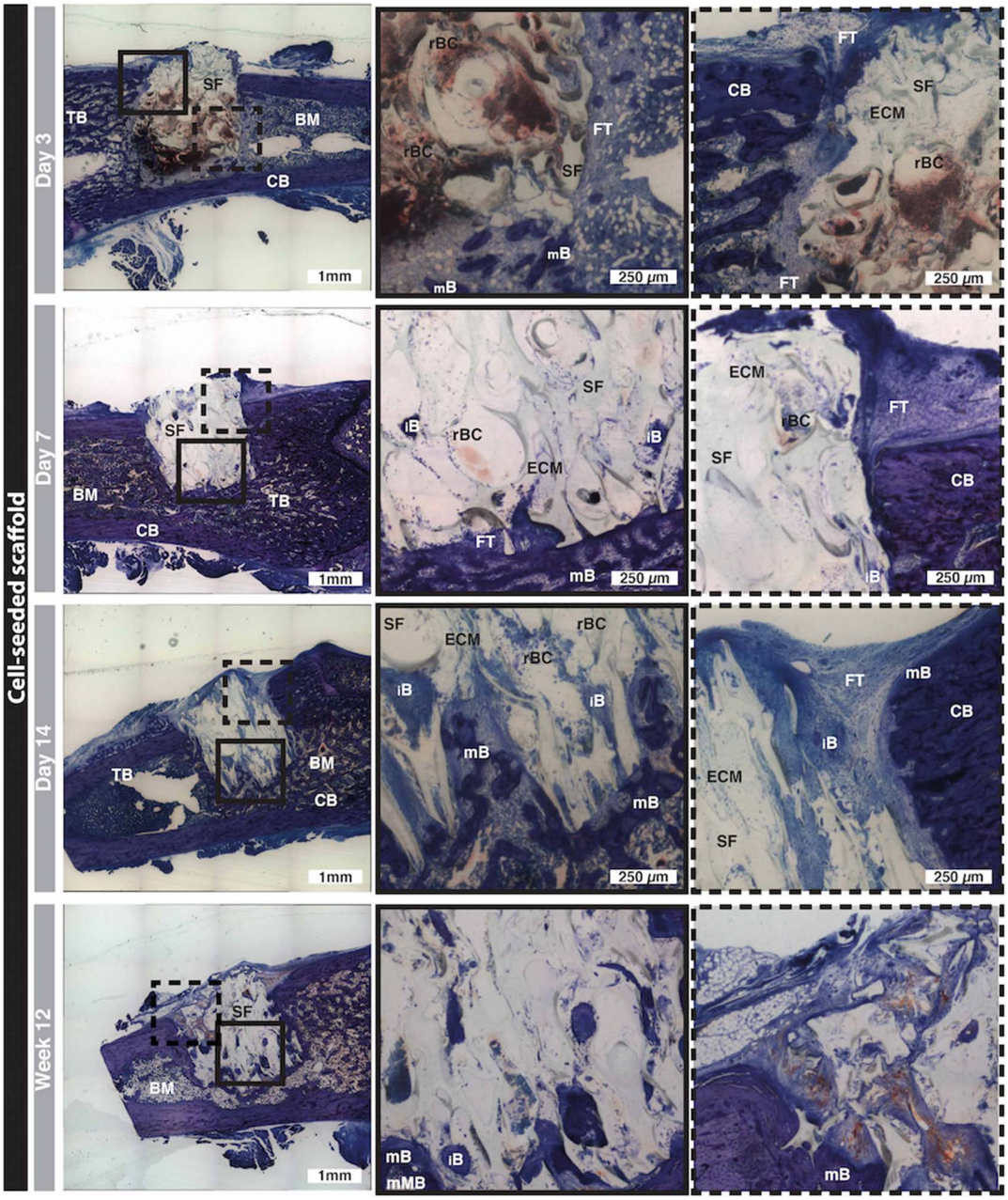

Figure 4. Toluidine blue-stained sections of CS scaffolds after 3, 7, and 14 days and after 12 weeks of implantation. TB, trabecular bone; CB, cortical bone; BM, bone marrow; SF, scaffold; rBC, red blood cells; FT, fibrous tissue; ECM, extracellular matrix; iB, immature bone; mB, mature bone modeling; CS, scaffold seeded with hBPCs; hBPCs, human bone progenitor cells.

CS scaffolds, one can see the extracellular matrix of the implanted cells, which is totally absent in the implanted CF scaffolds after 3, 7, and 14 days of implantation (Figs. 3 and 4). Immature bone started to grow inside the scaffold after 7 days and started to mineralize after 14 days of implantation for the implanted OCS, CS, and CF scaffolds. In the later case, the mineralization process was more pronounced and evolved than in the two other conditions. After 12 weeks of implantation, totally mature bone and active BM were observed in the CF scaffolds, whereas the bone maturity and BM activity in the CS and OCS scaffolds were less advanced and in a more immature state.

DISCUSSION

The use of hBPCs for BTE has been demonstrated to be promising[17,19]. As a xenograft tissue engineering scaffold is implanted in immunocompetent rats, the aim of

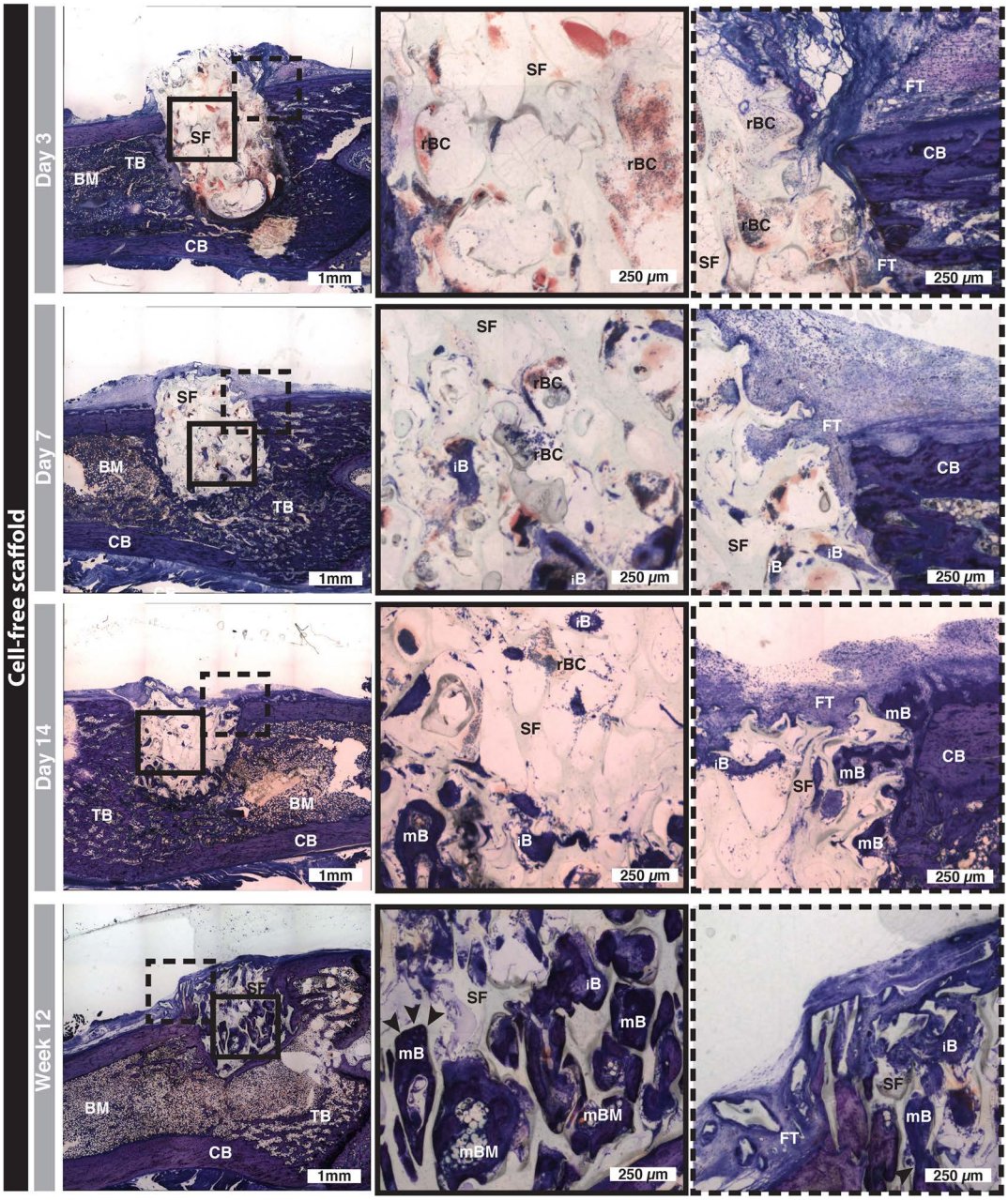

Figure 5. Toluidine blue-stained sections of CF scaffolds after 3, 7, and 14 days and after 12 weeks of implantation. TB, trabecular bone; CB, cortical bone; BM, bone marrow; SF, scaffold; rBC, red blood cells; FT, fibrous tissue; ECM, extracellular matrix; iB, immature bone; mB, mature bone modeling; CF, cell-free scaffold.

this study was to evaluate in vivo the potential type of immune reaction triggered by hBPCs and hOBPCs at an early stage of implantation and on the long term. We therefore implanted the scaffolds in femoral condyles of rats and analyzed them after 3, 7, and 14 days and after 12 weeks of implantation. Key findings of this study were (1) the enhancement of fibrous tissue formation in the OCS and CS scaffolds compared to the CF scaffolds in the early stage of implantation, while all three types of scaffolds had a comparable amount of immune cells on site; (2) the lack of fibrous capsule around the CS and OCS scaffolds after 12 weeks of implantation; and (3) the remodeling of healthy bone tissue inside the CS and OCS scaffolds with a delay compared to CF on the long term.

We first localized and visualized in vivo hBPCs for the first time by using an Alu-ISH on resin slides after

having characterized their ability to differentiate into osteoblasts when cultured in vitro (Supplementary materials, Figs. S1–S3). On these slides, we observed that both hBPCs and hOBPCs were still on site after 4 and 14 days of implantation in vivo. Because of technical problems, a limited number of samples could be processed. Therefore, we could only draw qualitative information on the presence of hBPCs and hOBPCs in the implanted sites. Should a better scaffold processing for immunohistochemistry in PLA/5% β-TCP scaffolds be possible, it would be interesting to (1) evaluate the difference between hBPCs and hOBPCs in terms of localization and migration kinetics and (2) evaluate in a more precise way the immune reaction by targeting specific cytokines, growth factors, and extracellular matrix components.

We then performed differential leukocyte counts and histological evaluations. We showed that the implantation of hBPCs and hOBPCs in immunocompetent rats did not trigger any specific immune response, even if they initiated a temporal formation of fibrous tissue at an early stage of implantation.

For the hematological analysis, significant differences were observed between the different scaffold conditions after 7 and 14 days of implantation. The increase in percentage of lymphocytes was statistically significant in the OCS scaffolds compared to the CS and CF scaffolds, whereas the percentage of monocytes and nonsegmented and juvenile neutrophils showed the inverse behavior after 7 days of implantation. At the same time point, the segmented neutrophils showed a higher percentage for the CF scaffolds than for the CS and OCS scaffolds. After 14 days of implantation, the monocyte percentage was significantly lower for the CF scaffolds than for the two others types of scaffolds. Comparing the values of the different types of white blood cells with other publications[27–29], we found that they were within the normal range for Wistar and Sprague–Dawley rats, except for the monocyte values. As the percentage of monocytes had values in the same range at day 0 than after 3, 7, and 14 days, we considered that there was no acute hematological effect due to the implantation of CF, CS, and OCS scaffolds.

The histological evaluation clearly showed that the presence of the immune cells, such as neutrophils, macrophages, lymphocytes, plasma cells, and multinuclear giant cells, was rarely observed in all three conditions from 3 to 14 days of implantation, while fibrous tissue was seen with the CS and OCS scaffolds. We observed, as well, a higher fibrous tissue formation in OCS scaffolds compared to CS scaffolds. As the immune response and the skeletal system work closely together, the immune cells play a pivotal role in determining the in vivo fate of the implanted material by contributing either to its success by facilitating new bone formation or to its failure with the creation of an inflammatory fibrous tissue capsule[20,30]. The results obtained after 12 weeks of implantation indicate that the host's body overcame the fibrous tissue formation instead of encapsulating the xenograft BTE scaffold. The histological evaluation indicated that the time needed to remodel the fibrous tissue in bone tissue inside the CS and OCS scaffolds was expressed by less mature bone formation and BM activity after 12 weeks of implantation compared to the CF scaffolds. However, the fibrous tissue formation in the CS and OCS conditions at an early stage of implantation could be favored by another cellular mechanism or cellular secretion, which arose certainly from the implanted hBPCs themselves. As cell fate is a temporal, spatial, and mechanical interplay between cells, cytokines, and growth factors[6], it is merely impossible to describe the interaction of the implanted hBPCs and the surrounding rat tissue. A possible cue could be given in a study published by Safadi et al.[31]. They demonstrated that connective tissue growth factor (CTGF) was expressed in normal bone during active growth or modeling and that its expression increased during the matrix mineralization and proliferation of primary osteoblasts from neonatal rats. This expression increases during mineralization, and proliferation of primary osteoblast could be a plausible explanation for the observed higher increase in fibrous tissue in OCS scaffolds compared to CS scaffolds. Other publications described that this growth factor was important in osteogenesis but played rather a more relevant role in fibrogenesis[32,33]. Therefore, the temporal effect of secreted CTGF could cause the presence of formed fibrous tissue from hBPCs and hOBPCs. In order to demonstrate this hypothesis, further in vitro and in vivo studies would be needed. In the case of in vitro studies, CTGF secretion of hBPCs and hOBPCs could be compared to those of rat BPCs (rBPCs) and endothelial cells, first observed and described to secrete CTGF[34]. Furthermore, additional in vivo experiments should give proof that the insertion of BPCs influences the formation of fibrous tissue, by analyzing the effect of implanted scaffolds seeded with either rBPCs or osteogenic rBPCs in rats. If in this last experiment a lower amount of bone density was observed using different types of cells originating from rat, it would confirm that the PLA/5% β-TCP scaffold used in this study is a system having the required quality to be applied in clinics without cell therapy. If, on the other hand, this in vivo experiment would show a significant increase in bone density inside scaffolds seeded with rat-affiliated cells, a potential clinical application of hBPCs in humans could be reconsidered.

ACKNOWLEDGMENTS: The authors thank Sandra Jaccoud for technical assistance in cell culture and surgery, and the EPFL Histology Core Facility for the technical assistance, particularly Jessica Dessimoz. The authors declare no conflicts of interest.

REFERENCES

1. Muramatsu K, Doi K, Ihara K, Shigetomi M, Kawai S. Recalcitrant posttraumatic nonunion of the humerus: 23 patients reconstructed with vascularized bone graft. Acta Orthop Scand. 2009;74(1):95–7.
2. Al-Sayyad MJ, Abdulmajeed TM. Fracture of the anterior iliac crest following autogenous bone grafting. Saudi Med J. 2006;27(2):254–8.
3. Costa-Pinto AR, Reis RL, Neves NM. Scaffolds based bone tissue engineering: The role of chitosan. Tissue Eng Part B Rev. 2011;17(5):331–47.
4. Klenke FM, Liu Y, Yuan H, Hunziker EB, Siebenrock KA, Hofstetter W. Impact of pore size on the vascularization and osseointegration of ceramic bone substitutes *in vivo*. J Biomed Mater Res A 2008;85A(3):777–86.
5. Das A, Botchwey E. Evaluation of angiogenesis and osteogenesis. Tissue Eng Part B Rev. 2011;17(6):403–14.
6. Amini AR, Laurencin CT, Nukavarapu SP. Bone tissue engineering: Recent advances and challenges. Crit Rev Biomed Eng. 2012;40(5):363–408.
7. Rechenberg von B, Genot OR, Nuss K, Galuppo L, Fulmer M, Jacobson E, Kronen P, Zlinszky K, Auer JA. Evaluation of four biodegradable, injectable bone cements in an experimental drill hole model in sheep. Eur J Pharm Biopharm. 2013;85(1):130–8.
8. Gomez-Barrena E, Rosset P, Lozano D, Stanovici J, Ermthaller C, Gerbhard F. Bone fracture healing: Cell therapy in delayed unions and nonunions. Bone 2015;70:93–101.
9. Roshan-Ghias A, Arnoldi J, Procter P, Pioletti DP. In vivo assessment of local effects after application of bone screws delivering bisphosphonates into a compromised cancellous bone site. Clin Biomech. 2011;26(10):1039–43.
10. Boerckel JD, Kolambkar YM, Dupont KM, Uhrig BA, Phelps EA, Stevens HY, García AJ, Guldberg RE. Effects of protein dose and delivery system on BMP-mediated bone regeneration. Biomaterials 2011;32(22):5241–51.
11. Boerckel JD, Kolambkar YM, Stevens HY, Lin ASP, Dupont KM, Guldberg RE. Effects of in vivo mechanical loading on large bone defect regeneration. J Orthop Res. 2012;30(7):1067–75.
12. Black CRM, Goriainov V, Gibbs D, Kanczler J, Tare RS, Oreffo ROC. Bone tissue engineering. Curr Mol Biol Rep. 2015;1(3):132–40.
13. Connolly JF. Injectable bone marrow preparations to stimulate osteogenic repair. Clin Orthop Relat Res. 1995;313: 8–18.
14. Quarto R, Mastrogiacomo M, Cancedda R, Kutepov SM, Mukhachev V, Lavroukov A, Kon E, Marcacci M. Repair of large bone defects with the use of autologous bone marrow stromal cells. N Engl J Med. 2001;344(5): 385–6.
15. Krebsbach PH, Mankani MH, Satomura K, Kuznetsov SA, Robey PG. Repair of craniotomy defects using bone marrow stromal cells. Transplantation 1998;66(10):1272–8.
16. Serafini M, Sacchetti B, Pievani A, Redaelli D, Remoli C, Biondi A, Riminucci M, Bianco P. Establishment of bone marrow and hematopoietic niches in vivo by reversion of chondrocyte differentiation of human bone marrow stromal cells. Stem Cell Res. 2014;12(3):659–72.
17. Montjovent M-O, Burri N, Mark S, Federici E, Scaletta C, Zambelli P-Y, Hohlfeld P, Leyvraz PF, Applegate LL, Pioletti DP. Fetal bone cells for tissue engineering. Bone 2004;35(6):1323–33.
18. Krattinger N, Applegate LA, Bivier E, Pioletti DP, Caverzasio J. Regulation of proliferation and differentiation of human fetal bone cells. Eur Cell Mater. 2011;21:46–58.
19. Montjovent M-O, Mark S, Mathieu L, Scaletta C, Scherberich A, Delabarde C, Zambelli P-Y, Bourban P-E, Applegate LA, Pioletti DP. Human fetal bone cells associated with ceramic reinforced PLA scaffolds for tissue engineering. Bone 2008;42(3):554–64.
20. Yin X, Zetao C, Jiang C, Chengtie W. Osteoimmunomodulation for the development of advanced bone biomaterials. 10th World Biomaterials Congress; 2016 May 17–22; Montreal, Canada. Front Bioeng Biotechnol. 2016; 19(6):304–21. [Abstract].
21. Mathieu LM, Mueller TL, Bourban PE, Pioletti DP, Müller R, Månson JA. Architecture and properties of anisotropic polymer composite scaffolds for bone tissue engineering. Biomaterials 2006;27(6):905–16.
22. Roshan-Ghias A, Terrier A, Bourban P-E, Pioletti DP. *In vivo* cycling loading as potent stimulatory signal for bone formation inside tissue engineering scaffolds. Eur Cell Mat. 2010;19:41–9.
23. Roshan-Ghias A, Lambers FM, Gholam-Rezaee M, Müller R, Pioletti DP. *In vivo* loading increases mechanical properties of scaffold by affecting bone formation and bone resorption rates. Bone 2011;49(6):1357–64.
24. Kettenberger U, Ston J, Thein E, Procter P, Pioletti DP. Does locally delivered Zoledronate influence peri-implant bone formation?—Spatio-temporal monitoring of bone remodeling *in vivo.* Biomaterials 2014;35(37):9995–10006.
25. Sflomos G, Dormoy V, Metsalu T, Jeitziner R, Battista L, Scabia V, Raffoul W, Delaloye J-F, Treboux A, Fiche M, Vilo J, Ayyanan A, Brisken C. A preclinical model for ERα-positive breast cancer points to the epithelial microenvironment as determinant of luminal phenotype and hormone response. Cancer Cell 2016;29(3):407–22.
26. Schormann W, Hammersen FJ, Brulport M, Hermes M, Bauer A, Rudolph C, Schug M, Lehmann T, Nussler A, Ungefroren H, Hutchinson J, Fändrich F, Petersen J, Wursthorn K, Burda MR, Brüstle O, Krishnamurthi K, von Mach M, Hengstler JG. Tracking of human cells in mice. Histochem Cell Biol. 2008;130(2):329–38.
27. Montjovent M-O, Mathieu L, Schmoekel H, Mark S, Bourban P-E, Zambelli P-Y, Laurent-Applegate LA, Pioletti DP. Repair of critical size defects in the rat cranium using ceramic-reinforced PLA scaffolds obtained by supercritical gas foaming. J Biomed Mater Res A 2007;83A(1):41–51.
28. Dyer SM, Cervasio EL. An overview of restraint and blood collection techniques in exotic pet practice. Vet Clin North Am Exot Anim Pract. 2008;11(3):423–43.
29. Gupta A, Liberati TA, Verhulst SJ, Main BJ, Roberts MH, Potty AGR, Pylawka TK, El-Amin SFI. Biocompatibility of single-walled carbon nanotube composites for bone regeneration. Bone Joint Res. 2015;4(5):70–7.
30. Miron RJ, Bosshardt DD. OsteoMacs: Key players around bone biomaterials. Biomaterials 2016;82:1–19.
31. Safadi FF, Xu J, Smock SL, Kanaan RA, Selim A-H, Odgren PR, Marks SC, Owen TA, Popoff SN. Expression of connective tissue growth factor in bone: Its role in osteoblast

proliferation and differentiation in vitro and bone formation *in vivo*. J Cell Physiol. 2003;196(1):51–62.
32. Moussad EE, Brigstock DR. Connective tissue growth factor: What's in a name? Mol Genet Metab. 2000;71(1–2):276–92.
33. Lee CH, Shah B, Moioli EK, Mao JJ. CTGF directs fibroblast differentiation from human mesenchymal stem/stromal cells and defines connective tissue healing in a rodent injury model. J Clin Invest. 2010;120(9):3340–9.
34. Bradham DM. Connective tissue growth factor: A cysteine-rich mitogen secreted by human vascular endothelial cells is related to the SRC-induced immediate early gene product CEF-10. J Cell Biol. 1991;114(6):1285–94.